HHS Public Access

Author manuscript

Curr Res Biotechnol. Author manuscript; available in PMC 2023 July 20.

Published in final edited form as:

Curr Res Biotechnol. 2023 ; 5: . doi:10.1016/j.crbiot.2023.100133.

CRISPR-based gene editing of non-homologous end joining factors biases DNA repair pathway choice toward single-strand annealing in *Aedes aegypti*

Keun Chae[a], **Justin M. Overcash**[b], **Chanell Dawson**[a], **Collin Valentin**[a], **Hitoshi Tsujimoto**[a], **Kevin M. Myles**[a], **Zach N. Adelman**[a,*]

[a]Department of Entomology, Texas A&M University, College Station, TX 77843, United States

[b]U.S. Department of Agriculture-Animal and Plant Health Inspection Service (USDA-APHIS), Biotechnology Regulatory Services, Riverdale, MD 20737, United States

Abstract

To maintain genome stability, eukaryotic cells orchestrate DNA repair pathways to process DNA double-strand breaks (DSBs) that result from diverse developmental or environmental stimuli. Bias in the selection of DSB repair pathways, either non-homologous end joining (NHEJ) or homology-directed repair (HDR), is also critical for efficient gene editing and for homing-based gene drive approaches developed for the control of disease-transmitting vector mosquitoes. However, little is understood about DNA repair homeostasis in the mosquito genome. Here, we utilized CRISPR/Cas9 to generate indel mutant strains for core NHEJ factors *ku80*, *DNA ligase IV* (*lig4*), and *DNA-PKcs* in the mosquito *Aedes aegypti* and evaluated the corresponding effects on DNA repair. In a plasmid-based assay, disruption of *ku80* or *lig4*, but not *DNA-PKcs*, reduced both NHEJ and SSA. However, a transgenic reporter strain-based test revealed that those mutations significantly biased DNA repair events toward SSA. Interestingly, *ku80* mutation also significantly increased the end joining rate by a yet-characterized mechanism in males. Our study provides evidence that the core NHEJ factors have an antagonistic effect on SSA-based DSB repair of the *Ae. aegypti* genome. Down-modulating the NHEJ pathway can enhance the efficiency of nuclease-based genetic control approaches, as most of those operate by homology-based repair processes along with extensive DNA end resection that is antagonized by NHEJ.

*Corresponding author. zachadel@tamu.edu (Z.N. Adelman).

Declaration of Competing Interest

The authors declare that they have no known competing financial interests or personal relationships that could have appeared to influence the work reported in this paper.

CRediT authorship contribution statement

Keun Chae: Conceptualization, Formal Analysis, Writing – original draft, Writing – review & editing. **Justin M. Overcash:** Investigation, Writing – review & editing. **Chanell Dawson:** Investigation, Writing – review & editing. **Collin Valentin:** Investigation, Writing – review & editing. **Hitoshi Tsujimoto:** Investigation. **Kevin M. Myles:** Writing – review & editing. **Zach N. Adelman:** Conceptualization, Formal Analysis, Writing – review & editing.

Appendix A. Supplementary material

Supplementary data to this article can be found online at https://doi.org/10.1016/j.crbiot.2023.100133.

Keywords

Aedes aegypti ; Eukaryotic DNA repair; DNA double-strand breaks; Genetic engineering

1. Introduction

Eukaryotic genomes are exposed to genotoxic stress from both metabolism and exogenous environmental causes: reactive oxygen species (ROS) (Winterbourn, 2008), DNA replication errors/stalled replication forks, inadvertent cleavage by abortive topoisomerase reactions (Pommier et al., 2016), V(D)J recombination and immunoglobulin heavy chain class switch recombination (CSR) (Soulas-Sprauel et al., 2007), and ionizing radiation and genotoxic compounds such as chemotherapeutic cancer treatments (Jeggo et al., 2016). For the maintenance of genome integrity, highly orchestrated DNA damage responses (DDRs) govern DNA lesion sensing, signaling cascades, chromatin remodeling, cell cycle checkpoints, and recruiting DNA repair proteins to coordinate DNA repair mechanisms (Huang and Zhou, 2020; Jackson and Bartek, 2009). DNA double-strand breaks (DSBs) are the most destructive challenge to genome integrity and cell fates, and therefore any failure in fixing them can lead to cancer development (tumorigenesis), aging, and cell death (apoptosis) (Alhmoud et al., 2020).

In eukaryotes, DSBs are mainly repaired by two distinct, antagonistic pathways: canonical non-homologous end joining (c-NHEJ) and homology-directed repair (HDR) (Chang et al., 2017; Marini et al., 2019). C-NHEJ is a constitutively active mechanism throughout all phases of the cell cycle. The heterodimer Ku70-Ku80 complex (KU) initially forms a protein ring that encircles the DNA helix at the DSB site with high affinity (Fell and Schild-Poulter, 2015; Walker et al., 2001), and subsequent phosphorylation activity of DNA-PKcs facilitates Artemis to process the broken DNA ends (Goodarzi et al., 2006). The final step is to fill in the gaps by DNA Pol X family polymerases (Pol μ and λ) (McElhinny et al., 2005) and reconnect them by the XLF-XRCC4-DNA Ligase IV (Lig4) complex (Brouwer et al., 2016; Grawunder et al., 1997). The c-NHEJ mechanism directly ligates the broken DNA ends and is intrinsically an error-free repair pathway in particular at endonuclease-triggered DSBs (Bétermier et al., 2014). As c-NHEJ is also versatile for non-compatible ends and does not require a template sequence, it often terminates the repair process by leaving sequence errors with nucleotide insertions or deletions (indels), especially being error-prone if DSBs would be repetitively triggered by the prolonged nuclease activity (Bétermier et al., 2014). In contrast, HDR repairs the DSB damage by the conversion of the sister chromosome or homologous chromosome as the template, which leads to error-free recovery and/or loss of heterozygosity. However, the activity of this repair pathway is restricted to late S and G2 phases when sister chromatids are available (Ovejero et al., 2020). Unlike c-NHEJ, the HDR pathway requires extensive DNA end resection (the 5′-to-3′ nucleolytic process at the DSB site), generating long 3′-single-stranded DNA (3′-ssDNA) tails (Symington and Gautier, 2011). Mre11 of the MRN (Mre11-Rad50-NBS1) complex, in association with CtIP, generates short 3′-ssDNA tails in the proximity of the DSB site (Cannavo and Cejka, 2014; Sartori et al., 2007; Shibata et al., 2014). This resection process is further extended by Exo1 and Dna2 with a helicase activity of BLM, resulting in extensive lengths of 3′-ssDNA

tails (Nimonkar et al., 2011), which are coated and stabilized by the ssDNA binding protein, RPA (Chen et al., 2013). BRCA2, recruited by interactions with BRCA1-PALB2-BARD1, facilitates replacing RPA with RAD51 and promotes RAD51 filament formation, which leads to strand invasion of homologous DNA strands by forming the D loop (Sun et al., 2020).

In addition to c-NHEJ and HDR, DSBs are also repaired by two other alternative pathways: single-strand annealing (SSA) and the alt-EJ/MMEJ pathway. SSA deletes whole segments of DNA when DSBs occur between two identical sequence motifs, known as direct repeats (DRs) (Bhargava et al., 2016). Although SSA is highly mutagenic, it is considered a type of homology-based DNA repair because it requires extensive end resection (Bhargava et al., 2016). RAD52 scans RPA-coated ssDNA tails for strand homology and facilitates cleavage and annealing activity of the XPF-ERCC1 endonuclease complex (Motycka et al., 2004). The alt-EJ/MMEJ pathway is a PARP1-dependent, error-prone mechanism that can be activated in the absence of Ku-dependent NHEJ (Cheng et al., 2011; Decottignies, 2007; Wang et al., 2006). PARP1 forms a platform for other factors including DNA polymerase θ (Pol θ) and Lig1 or Lig3 (Gibson and Kraus, 2012; Masani et al., 2016; Mateos-Gomez et al., 2015). Unlike c-NHEJ, alt-EJ requires MRN/CtIP for short 5′-resections of the DSB ends, which provides micro-homologous sequence repeats (<20 bp) like a small-scaled SSA event (Decottignies, 2007).

Understanding DSB repair pathway selection mechanisms, especially between c-NHEJ and HDR, is critical for developing nuclease-associated genome editing technologies for controlling disease-transmitting mosquito vectors. Many genetics-based population control approaches are based on the activity of transgenic components such as nucleases or effectors (Raban et al., 2020). Especially for a nuclease-based technology, how the DSB is processed and by which pathway heavily influences its potential to spread in the target population. For example, a CRISPR/Cas9-triggered, homing-based gene drive approach requires efficient HDR-mediated transgene conversion into the wild-type sister chromosome (Raban et al., 2020). A self-eliminating transgene technology works by skewing DSB repair toward the SSA pathway, a subtype of HDR (Chae et al., 2022; Zapletal et al., 2021). The key mode of action for both mechanisms is the presence of long 3′-ssDNA tails of the homologous sequences, which can be produced only by an extensive end resection process (Marini et al., 2019). Thus, down-modulating the Ku-associated NHEJ pathway that antagonizes DNA end resection is expected to promote homology-based repair processes and thereby enhance the efficiency of nuclease-based genetic control approaches. In fact, NHEJ-driven indel mutations are predicted to negatively influence the ability of homing-based gene drives to spread into populations (KaramiNejadRanjbar et al., 2018).

In this study, we attempted to characterize roles of the core NHEJ factors in processing DSBs that are locally induced by nucleases in the *Aedes aegypti* genome. First, CRISPR/Cas9-mediated gene editing established indel mutant strains of three critical NHEJ factors (Ku80, Lig4, and DNA-PKcs). Subsequentially, individual mutant strains were evaluated for DSB repair pathway-associated marker phenotypes in three independent reporter systems: (i) plasmid-based reporters, DSBs induced by I-*Ani*I; (ii) a transgene-based reporter, DSBs induced by I-*Sce*I (Chae et al., 2022); (iii) *kmo*-targeted DNA repair, DSBs induced by

CRISPR/Cas9. Our assay results suggest that *Ae. aegypti* NHEJ factors compete with SSA, mechanisms that could be further adapted for genome engineering technologies.

2. Materials and methods

2.1. Mosquito rearing and microinjection

All *Ae. aegypti* strains were based off of the Liverpool (*Lvp*) wild-type strain and were maintained at 27°C and 70% (±10%) relative humidity, with a day/night cycle of 14 hr light and 10 hr dark. Larvae were fed powdered fish food (TetraMin Tropical Flakes), and adult mosquitoes were fed 10% sucrose solution. The mated females were fed on defibrinated sheep blood (Colorado Serum Company) using an artificial membrane feeder. For the microinjection procedure, female mosquitoes at three to four days post-bloodmeal were placed in a 50 ml conical tube with a wet filter paper and kept in the dark for 45 min for oviposition. Fresh embryos were aligned on a double-sided taped coverslip, and the developing embryos at the pre-blastoderm stage were injected at the posterior pole through a beveled capillary needle with an injection mix as previously described (Basu et al., 2016; Kistler et al., 2015).

2.2. Generation of CRISPR/Cas9-driven indel mutant strains

For CRISPR/Cas9-based gene editing, *Lvp* embryos were microinjected using a solution containing 0.4 μg/μl of CRISPR/Cas9 enzyme (PNA Bio) and 0.1 μg/μl of sgRNAs (Supplementary Table S1); the latter of which were transcribed *in vitro* using MEGAscript T7 Transcription Kit (Ambion). The injection mix was incubated at 37°C for 20 min prior to microinjection to allow for the formation of CRISPR/Cas9-sgRNA complexes. Surviving G_0 mosquitoes were outcrossed with *Lvp*, and individual G_1 mosquitoes were examined for CRISPR-generated indel mutations by high-resolution melt analysis (HRMA) using the Phire Animal Tissue DirectPCR Kit (Thermo Scientific). The list of HRMA primers is presented in Supplementary Table S2.

2.3. The reporter plasmid-based DNA repair test

Three reciprocal parental crosses were set up between the *trans*-heterozygous indel mutant (*ku80*$^{-/-}$, *lig4*$^{-/-}$, or *DNA-PKcs*$^{-/-}$) and *Lvp* strains; 1) ♂ *gene*$^{-/-}$ x ♀ *gene*$^{-/-}$; 2) ♂ *Lvp* × ♀ *gene*$^{-/-}$; 3) ♂ *Lvp* × ♀ *Lvp*. Eight replicates (n = 50 embryos per each) of each embryo group were microinjected with the luciferase reporter plasmid for either NHEJ or SSA assay (pNHEJ2.1 or pSSA, 0.5 μg/μl), together with a normalization control plasmid (pSLfa-PUb-Renilla, 0.2 μg/μl) and a plasmid coding for the homing endonuclease (pY2-I-*Ani*I, 0.2 μg/μl). For negative controls, pY2-I-*Ani*I was replaced by a blank plasmid (pSLfa-mcs, 0.2 μg/μl) for microinjections. All injected embryos were incubated at 27°C in a humidity chamber for 48 hr post-injection, and the collected embryos were kept at −80°C until further analysis. The DNA repair event-dependent luciferase activity in each embryo group was measured by using the Dual-Luciferase Reporter Assay System (Promega) and the SpectraMax MiniMax 300 Imaging Cytometer (Molecular Devices).

2.4. The reporter strain-based DNA repair test

To evaluate effects of NHEJ-associated gene disruption on the SSA-driven transgene elimination (Chae et al., 2022), each indel mutant strain (*ku80*$^{-/-}$, *lig4*$^{-/-}$, or *DNA-PKcs*$^{-/-}$) was crossed with either the reporter strain (*kmo*^{RG}) or the nuclease-expressing strain (*nos-I-SceI*). Through HRMA-based genotyping analysis and fluorescent marker screening, we obtained two types of double-mutant strains (*gene*$^{-/-}$/*kmo*^{RG} and *gene*$^{-/-}$/*nos-I-SceI*) and set up reciprocal crosses between them as previously described (Chae et al., 2022). F_1 progeny (white-eye; EGFP+; DsRED+; BFP+) were outcrossed with the *kmo*$^{-/-}$ strain. Female mosquitoes were blood-fed twice, and all embryos were hatched for F_2 larval screening for DNA repair pathway-dependent marker phenotypes. In addition to collective screening, individual F_1 female mosquitoes were allowed to produce F_2 embryos by using the 24-well plate-based oviposition method (Tsujimoto and Adelman, 2021). Each F_2 pool of larvae was independently screened for DNA repair variation or bias originating from a single mosquito.

2.5. The kmo-targeted DNA repair test

A *kmo*-targeting plasmid donor, pBR-KmoEx4 (Chae et al., 2022), was injected to three embryo groups (~800 to ~ 1,200 per group) with various maternal levels of the NHEJ-associated gene (null/heterozygous/WT), descended from reciprocal parental crosses between the indel mutant (*ku80*$^{-/-}$, *lig4*$^{-/-}$, or *DNA-PKcs*$^{-/-}$) and *Lvp* strains. The injection mix included 0.2 μg/μl of pBR-KmoEx4, 0.4 μg/μl of CRISPR/Cas9 enzyme (PNA Bio), and 0.1 μg/μl of sgRNA-KmoEx4 (Chae et al., 2022). Surviving G_0 mosquitoes were outcrossed with the *kmo*$^{-/-}$ strain, which contains a TALEN-generated *kmo*-null mutant allele (Aryan et al., 2013a), phenocopying the *kh*^{w} strain (Cornel et al., 1997). G_1 larvae were screened for DNA repair event-dependent phenotypes of eye color and marker expression; white eye (Kmo-) is caused by end joining mechanisms, and the EGFP fluorescent body (Kmo-; EGFP+) is caused by the homology-directed repair mechanism.

2.6. Quantitative real-time PCR (qRT-PCR) for gene expression levels in embryos

For RNA extraction, embryos (n = ~200) were collected at 48 h after crosses of 1) male mutant × female mutant; 2) male WT × female mutant; 3) male WT × female WT. The embryos were homogenized using a disposable pestle (Kontes) in TRIzol reagent (Thermo Fisher), and total RNA was extracted by following the manufacturer's protocol (rinsed with 75% ethanol two times) and further treated by DNase (TURBO DNA-*free* kit, Thermo Fisher) at 37 °C for 1 h. For cDNA synthesis, 1 μg of the total RNA per sample was used with oligo $d(T)_{20}$-VN primers and Superscript IV (Thermo Fisher). The reactions were incubated at 50 °C for 50 min and the reverse transcriptase was inactivated at 80 °C for 10 min. A 1/50 dilution of the cDNA was used for qRT-PCR. We used Primer3 (Untergasser et al., 2012) to design gene-specific primer pairs for individual NHEJ genes (Supplementary Table S2). Prior to using Primer3, the target sequences were subjected to Mfold (Zuker, 2003) to predict secondary structures at the expected annealing temperature (60 °C) to exclude such regions from primer annealing sites. The primers were empirically verified for optimal annealing temperature range and amplification efficiency (E) using a serial dilution of cDNA templates. All primer pairs were determined to have E between 95 and 105 (in %). qRT-PCR reactions were run on Bio-Rad CFX96 and SsoAdvanced Universal SYBR Green

Supermix (Bio-Rad) with the thermal cycle of 95 °C for 30 s and 45 cycles of 95 °C for 15 s and 57 °C for 30 s followed by melt analysis between 65 and 95 °C. All the reactions were performed in triplicated wells.

3. Results

3.1. Generation of CRISPR/Cas9-driven indel mutant mosquito strains for NHEJ-associated genes in Ae. aegypti

To further understand DNA repair choice in *Ae. aegypti*, we proceeded to disrupt functions of three core genes in the NHEJ pathway: *ku80*, *DNA ligase IV* (*lig4*), and *DNA-PKcs* by utilizing CRISPR-mediated mutagenesis. For the *ku80* genomic locus, we designed two clusters of sgRNAs (Fig. 1A; Supplementary Table S1). The sgRNA site #1 targeting exon 3 is predicted to disrupt the N-terminal α/β domain [Pfam: PF03731 (Finn et al., 2016)], while site #2 targets exon 4 to truncate the Ku80 protein at the β-barrel domain [Pfam: PF02735 (Finn et al., 2016)] that is critical for DNA binding (Walker et al., 2001). High-resolution melt analysis (HRMA) following microinjection (4 replicates of 50 embryos), showed that sgRNAs targeting site #2 displayed higher DSB-inducing activity than the site #1 group (Table 1). With the use of the site #2 group, we obtained two deletion alleles, *ku*80$^{\Delta 1/+}$ and *ku*80$^{\Delta 8/+}$, whose intercross was able to produce *trans*-heterozygous indel mutant mosquitoes (*ku*80$^{\Delta 1/\Delta 8}$) (Fig. 1A; Supplementary Fig. S1A).

For the *lig4* gene, the sgRNA lig4–3, tested in a previous study (Basu et al., 2015), was predicted to efficiently truncate the mature protein including the BRCT domain [InterPro: IPR036420 (Blum et al., 2021)], which interacts with XRCC4 (Wu et al., 2009), was utilized in this study for microinjections (Fig. 1B; Supplementary Table S1). We identified two mutations of nucleotide deletions ($\Delta 7^{M}$ and $\Delta 11^{M}$) targeted at the sex chromosome-like M−linked *lig4* allele and three mutations of nucleotide deletion ($\Delta 2^{m}$, $\Delta 5^{m}$, and $\Delta 7^{m}$) targeted at the m-linked *lig4* allele in G_1 HRMA (Table 1). Three indel mutant lines (*lig4*$^{M\Delta 11/m+}$, *lig4*$^{m\Delta 2/m+}$, and *lig4*$^{m\Delta 7/m+}$) were further utilized to establish the *trans*-heterozygous group (*lig4*$^{M\Delta 11/m\Delta 2/m\Delta 7}$) for functional analysis in this study (Supplementary Fig. S1 B to D).

To inactivate the *DNA-PKcs* gene in *Ae. aegypti*, we targeted four sgRNA areas in exon 5, which would truncate the mature protein by disrupting major motifs such as ARM: Armadillo-type fold [InterPro: IPR016024 (Blum et al., 2021)], FAT (FRAP, ATM and TRRAP): a novel domain in phosphatidylinositol kinase (PIK)-related kinases [Pfam: PF02259 (Finn et al., 2016)], and PI3-/4-kinase catalytic domain [Pfam: PF00454 (Finn et al., 2016)] (Fig. 1C; Supplementary Table S1). Through microinjections of the CRISPR system, we obtained four indel mutations, nucleotide insertion (+5 bp) or deletions (Δ7, Δ10, or Δ38 bp), by using sgRNA#3 and #4 groups in G_1 HRMA (Table 1). Two indel mutant strains, *DNA-PKcs*$^{\Delta 10/+}$ and *DNA-PKcs*$^{\Delta 38/+}$, were further maintained to establish the *trans*-heterozygous group (*DNA-PKcs*$^{\Delta 10/\Delta 38}$) for functional study (Fig. 1C; Supplementary Fig. S1E).

In these CRISPR-based indel mutant strains, mRNA levels were not suppressed in embryos compared to the wild type (Supplementary Table S3). This was not surprising, as none

of the indels introduced are in proximity to the initiation of translation, where nonsense-mediated decay might be triggered. This suggests that any mutant phenotype would be associated with a change in the protein level or quality, though we lack the mosquito-specific antibodies required to address this directly. Additionally, we do not exclude the possibility that phenotypic abnormality can be caused by the aberrant activity of truncated proteins, which accumulate by premature termination of translation due to the out-of-frame indel formation (Fig. 1). This mutation effect can be associated with a loss of a specific protein motif or active domain in individual NHEJ factors. Regardless of mutant nature, we use the genotypic nomenclatures in this study like '*gene*$^{-/-}$', '*gene*$^{+/-}$', and '*gene*$^{+/+}$', such that the plus superscript (+) designates the presence of the intact wild-type allele and the minus superscript (−) designates its absence due to any mutagenic disruption. Hereafter, we refer to the *trans*-heterozygous mosquito strain as '*gene*$^{-/-}$' because generational maintenance results in genotypic variations of indel alleles within the group. For example, *ku80*$^{-/-}$ indicates the group of *ku*80$^{\Delta1/\Delta8}$, *ku*80$^{\Delta1/\Delta1}$, and *ku*80$^{\Delta8/\Delta8}$. Likewise, *DNA-PKcs*$^{-/-}$ indicates the group of *DNA-PKcs*$^{\Delta10/\Delta38}$, *DNA-PKcs*$^{\Delta10/\Delta10}$, and *DNA-PKcs*$^{\Delta38/\Delta38}$. The *lig4* gene is linked to the sex locus, by which males and females have distinct mutant alleles. Therefore, *lig4*$^{-/-}$ indicates the male group of *lig4*$^{M\Delta11/m\Delta2}$ and *lig4*$^{M\Delta11/m\Delta7}$ and the female group of *lig4*$^{m\Delta2/m\Delta7}$, *lig4*$^{m\Delta2/m\Delta2}$, and *lig4*$^{m\Delta7/m\Delta7}$.

3.2. Ae. aegypti ku80 and lig4, but not DNA-PKcs, are indispensable for repairing DSBs on reporter plasmids in early embryo development

To determine the effects of CRISPR/Cas9-driven indel mutation at NHEJ-associated genes on DNA repair, we developed a reporter plasmid with EGFP fused to an out-of-frame luciferase gene. DSB-induction by the endonuclease I-*Ani*I followed by mutagenic NHEJ-based repair should result in the shifting of the luciferase coding region to in-frame and thus activation of luc activity (Fig. 2A). The reporter plasmid was microinjected, with or without a DSB-inducer plasmid (pY2-I-*Ani*I) along with a Renilla-luc control plasmid (Aryan et al., 2013b) into pre-blastoderm embryos in 8 replicates of 50 embryos oviposited from three reciprocal crosses: 1) ♂ *nhej*$^{-/-}$ x ♀ *nhej*$^{-/-}$; 2) ♂ *Lvp* × ♀ *nhej*$^{-/-}$; 3) ♂ *Lvp* × ♀ *Lvp*. At 48 hr post-injection, NHEJ-dependent DSB repair was measured by a dual-luciferase assay (Fig. 2 B–D). As expected, disruption of *ku80* eliminated luciferase activation, suggesting DSBs were either not repaired, or were repaired without errors, whereas mutagenic repair was readily observed in wild-type controls (Fig. 2B). Interestingly, disruption of maternal *ku80* was sufficient to abrogate repair. Similar results were obtained for *lig4* mutant alleles, though heterozygous individuals exhibited normal repair in this case (Fig. 2C). In contrast, no change in repair outcomes was observed in *DNA-PKcs* mutant alleles, indicating DNA-PKcs is dispensable for repair of the injected plasmid DNA (Fig. 2D).

To determine the effects of each gene disruption on homology-based repair, we utilized a previously generated plasmid reporter, termed here pSSA (Fig. 2E) designed to activate firefly luciferase following SSA-based repair of an induced DSB (Aryan et al., 2013b). Embryos of each genotype were injected with the test reporter along with a Renillaluc control reporter and a source of I-*Ani*I, and the degree of luciferase activation was determined. Surprisingly, mutant alleles of *ku80* also reduced activation of the SSA reporter (Fig. 2F), as did *lig4* mutation, albeit to a lesser and more ambiguous extent (Fig. 2G).

As with the NHEJ reporter, mutant alleles of *DNA-PKcs* had no effect on the activity of the SSA reporter (Fig. 2H). The down-modulating effect of *ku80* and *lig4* gene mutations on SSA was unexpected, given the antagonistic nature of the NHEJ pathway against end resection processing that is the rate-limiting step for HDR and SSA (An et al., 2018; Canny et al., 2018). It is possible that results from the SSA reporter plasmid assay may reflect an alternative end joining (alt-EJ) event such as microhomology-mediated end joining (MMEJ), which can be activated in the absence of Ku proteins (Mansour et al., 2013).

3.3. A transgenic reporter-based assay to detect SSA and NHEJ repair events in Ae. aegypti

Previously, we showed that the SSA pathway in *Ae. aegypti* can result in the removal of transgenic cargo genes when flanked by two identical sequences, known as direct repeat (DR) motifs (Aryan et al., 2013b). More recently, we engineered fluorescent reporter genes at the *kmo* gene locus in an arrangement which allow us to determine what pathway was selected for DNA repair, based upon marker phenotypes (Chae et al., 2022) (Supplementary Fig. S2). The engineered strain, kmo^{RG} (white eye; DsRED+; EGFP+), contains a DsRED transgene engineered with an I-*Sce*I recognition site at the start codon, as well as an EGFP marker gene, both integrated into the coding region of the *kmo* gene critical for eye pigmentation (Han et al., 2003). Additionally, both reporter genes are collectively flanked by DR sequences corresponding to the *kmo* gene region. A source of the I-*Sce*I endonuclease is provided by a second strain, *nos-I-SceI* (white eye; BFP+), which contains the eye-specific BFP marker gene with a genetic background of $kmo^{-/-}$ (Aryan et al., 2013a) and expresses I-*Sce*I under germline-specific *nos* promoter activity (Adelman et al., 2007). When these two strains are parentally crossed, I-*Sce*I-induced DSBs occur on DsRED in F_1 offspring mosquitoes, and the type of DSB repair mechanism, either NHEJ or SSA, utilized for repairing the DSBs can be identified based upon marker phenotypes in the F_2 offspring.

The SSA pathway is known to require an extensive resection process of the damaged sequence, which is antagonized by the NHEJ pathway (An et al., 2018; Liu and Huang, 2016). Therefore, we hypothesized that disruption of NHEJ factors would lead to a decrease in NHEJ-triggered indels and an increase in SSA-based transgene elimination, which could be detected by our transgenic reporter system (Chae et al., 2022). To test this, we crossed each test strain into the indel mutant background of the respective NHEJ factor, resulting in genotypes $SceI/nhej^{-/-}$ and $kmo^{RG}/nhej^{-/-}$, which were crossed to generate an F_1 generation containing both factors (Fig. 3). We note that due to maternal effects provided by the *nos* promoter, nuclease-driven DSB induction will vary based on the crossing direction, while cellular levels of baseline NHEJ activity may vary based on the developmental stage of the mosquito. Specifically, we note three critical differences between the directionality of the crosses. First, when the males of genotype $SceI/nhej^{-/-}$ (the DSB inducer) are utilized for the parental cross (F_0), the I-*Sce*I nuclease is predicted to be expressed only after an early phase of the F_1 embryo (beginning of zygotic transcription). In contrast, the use of the female $SceI/nhej^{-/-}$ strain provides the nuclease from oocyte development, which allows DSB induction and its repair in the absence of the normal NHEJ factor from the formation of the zygote. Thus, phenotypic differences between the parental male ($F_0^{♂}$) and female ($F_0^{♀}$) groups could indicate mutant effects of individual NHEJ factors on DNA repair at an

early phase of the F_1 embryo. At the same time, phenotypic differences between the F_1^{δ} and F_1^{φ} groups can reflect differential effects of NHEJ gene disruption on DSB repair in male and female gametogenesis. Finally, in the F_2 generation, the outcross to the *kmo*-null strain (*kmo*$^{-/-}$/*nhej*$^{+/+}$) also restores at least one NHEJ^{+} allele, meaning that once zygotic transcription begins, NHEJ gene levels should be restored in all test conditions, with any phenotypic differences in reporter activity between cohorts reflecting repair prior to this timepoint. Taken together, the individual SSA test group reveals the roles of NHEJ genes in DNA repair in a specific window of developmental phases (Fig. 3): (i)$F_0^{\delta} - F_1^{\delta}$, from F_1 late embryo to F_1 adults; (ii)$F_0^{\delta} - F_1^{\varphi}$, from F_1 late embryo to F_2 early embryo; (iii)$F_0^{\varphi} - F_1^{\delta}$, from F_1 early embryo to F_1 adults; (iv)$F_0^{\varphi} - F_1^{\varphi}$, from F_1 early embryo to F_2 early embryo.

3.4. CRISPR-driven indel mutation of NHEJ factors significantly increased SSA frequency

For the reporter assay in the absence of the wild-type *ku80* gene (Fig. 4; Supplementary Table S4), we set up the parental cross by utilizing nuclease-expressing males (F_0: ♂ *ku80*$^{-/-}$/*nos-I-SceI*), but not females (♀ *ku80*$^{-/-}$/*nos-I-SceI*), as female *ku80*$^{-/-}$ mosquitoes did not produce sufficient numbers of embryos. In F_2 progeny of both $F_0^{\delta} - F_1^{\delta}$ and $F_0^{\delta} - F_1^{\varphi}$ crosses, the rate of SSA (% Blk/[WGR + WG + Blk]) was significantly increased by *ku80*$^{-/-}$, compared to the WT controls, suggesting a critical role of *ku80* in NHEJ antagonizing HDR-type repairs in *Ae. aegypti*. Interestingly while in the $F_0^{\delta} - F_1^{\delta}$ cross, the NHEJ rate (% WG/[WGR + WG + Blk]) also increased in *ku80*$^{-/-}$ as compared to WT, this was not observed through female F_1 adults ($F_0^{\delta} - F_1^{\varphi}$). This indicates that an alternative, error-prone DNA repair mechanism can be activated in the absence of the functional KU complex in a male germline-specific manner in *Ae. aegypti*.

In the F_2 generation from reciprocal crosses between *lig4*$^{-/-}$/*kmo*^{RG} and *lig4*$^{-/-}$/*nos-I-SceI* (Fig. 5A; Supplementary Tables S5 and S6), the rates of NHEJ in *lig4*$^{-/-}$ were not significantly different from those in the WT controls, for any of the four crossing schemes. Likewise, in the absence of maternally contributed I-*Sce*I, *lig4*$^{-/-}$ had no effect on the rate of SSA-based repair. In contrast, rates of SSA increased 3- to 4-fold more than those of WT when the DSB inducer (I-*Sce*I) was maternally provided from parental crosses ($F_0^{\varphi} - F_1^{\delta}$ and $F_0^{\varphi} - F_1^{\varphi}$). This suggests a critical role for *lig4* in DNA repair events following maternally triggered DSB damage at an early stage of the F_1 embryo. As these data were aggregated across pooled individuals, we also scored the DSB repair-associated marker phenotypes within each F_2 larval group per F_1 individual by allowing each F_1 female mosquito to oviposit embryos independently (Fig. 5B). *lig4*$^{-/-}$ did not increase the overall SSA rates per F_1 female, compared to those in WT. However, rates of SSA were significantly increased, compared to those of NHEJ, when DSBs were maternally triggered by females at either F_0 or F_1 ($F_0^{\varphi} - F_1^{\delta}$, $F_0^{\varphi} - F_1^{\varphi}$ and $F_0^{\delta} - F_1^{\varphi}$). We also quantified the capacity of F_1 adults to pass SSA or NHEJ phenotypes to their F_2 offspring (Fig. 5C). The ratio of SSA over NHEJ (% Blk/WG) increased in *lig4*$^{-/-}$, compared to WT controls, when DSBs were maternally triggered by F_0 females ($F_0^{\varphi} - F_1^{\delta}$ and $F_0^{\varphi} - F_1^{\varphi}$). In contrast, their difference in $F_0^{\delta} - F_1^{\varphi}$ (Fig. 5 B and C) may reflect an increased SSA rate during F_1 female gametogenesis. Thus, *Ae. aegypti lig4* appears to play a unique role in NHEJ, particularly in the early stages of embryo

development and potentially in oogenesis, while other factors or EJ pathways may be able to substitute for its activity at other stages.

In contrast to *ku80*$^{-/-}$ and *lig4*$^{-/-}$, when crosses were performed in a *DNA-PKcs*$^{-/-}$ genetic background, SSA rates were shown to be elevated 2- to 3-fold more than those of WT, regardless of the paternally ($F_0^{\male}$)- or maternally ($F_1^{\female}$)-provided nuclease gene from the parental crosses (Fig. 6A; Supplementary Tables S7 and S8). These results suggest that loss of DNA-PKcs may not be critical for DNA repair during the early phases of embryo development. A similar pattern of DNA repair bias was also found within individual families (Fig. 6B). However, *DNA-PKcs*$^{-/-}$ significantly increased the ratio of SSA over NHEJ (% Blk/WG) only in the $F_0^{\male}$ – $F_1^{\female}$ group (>2.5-fold) (Fig. 6C). This could be due to the suppression of NHEJ rates in this group, while all other groups had a similar level of enhancement for both SSA and NHEJ rates shown in F_1 (%). These results indicate that *DNA-PKcs* may have a regulatory role in DNA repair pathway choice in a developmental stage from late embryogenesis to gametogenesis when germline cells differentiate.

3.5. NHEJ factors participate in kmo-targeted DSB repair through diverse physiological responses yet to be identified in Ae. aegypti

In addition to its core function in homing-based gene drive (Alphey, 2014; DiCarlo et al., 2015; Esvelt et al., 2014; Gantz et al., 2015; Gantz and Bier, 2015), the HDR pathway is routinely utilized in the laboratory setting to deliver plasmid donor DNA to a targeted genomic locus, which generates a transgenic knock-in strain. We previously described dsRNA-based silencing of *ku70* coincident with microinjection enhanced the rates of transgene integration, providing evidence that the error-prone NHEJ pathway antagonizes HDR mechanisms in the *Ae. aegypti* genome (Basu et al., 2015). To further understand the effects of NHEJ on plasmid donor-based ectopic HDR, we microinjected the *kmo*-targeting plasmid (pBR-KmoEx4) with Cas9 protein and gRNA into three embryo groups (n > 800 per group) of each *nhej*$^{-/-}$ strain with 0, 1 or 2 copies of the relevant functional gene (Supplementary Fig. S3; Supplementary Tables S9 to S14). However, increased lethality and infertility of G_0 mosquitoes during the microinjection procedure in mutant strains as compared to WT contributed to few successful HDR events precluding effective comparisons. Instead, we focused on scoring NHEJ-associated indel phenotypes across each of the genotypes, where sample sizes were much larger. For instance, when maternal levels of *ku80* were lowered, the rates of indels increased at G_0, compared to WT. This inverse relationship indicates potential activation of an alternative end joining mechanism in the absence of Ku proteins (Mansour et al., 2013). Moreover, this uprise was strengthened at G_1 offspring and specific to males, supplementing our early observation that an alternative pathway may be responsible for an increase of indels in male germline development (Fig. 4). Unlike *ku80*, the levels of *lig4* in embryos appeared to be directly correlated with the rates of NHEJ, indicating that in *Ae. aegypti lig4* is essential for DNA repair mechanisms, especially in developing embryos as shown in Fig. 2. Unexpectedly, a high rate of indels occurred only with *DNA-PKcs* heterozygosity, and this outcome was strengthened at G_1 offspring. This also supplements other test results that DNA-PKcs was predicted to play a homeostatic role in a highly orchestrated manner during germline development (Fig. 6), but not in early embryos (Fig. 2).

4. Discussion

In our study, different parameters between the three assay types were considered for interpretating CRISPR-based gene editing and phenotype changes for distinct roles of individual NHEJ factors in DSB repair of *Ae. aegypti* (Fig. 7). First, in reporter strain-based tests, individual NHEJ gene disruption influenced DNA repair pathway selection mechanisms and thereby significantly enhanced the rates of SSA (Figs. 4 – 6). Phenotypes from reporter strain-based tests are relevant to germline-specific DSB repair events, which were induced by *nos* promoter-controlled nuclease activity at F_1 and passed over to F_2 offspring. Based on how the nuclease gene is provided (maternally or paternally), we dissected the distinct effects of NHEJ gene disruption on DSB repair. Phenotypic differences between F_1^{δ} and F_1^{φ} reflect genetic mutation effects of individual NHEJ factors on DSBs occurred in early (zygotic) embryos. Phenotypic differences between F_0^{δ} and F_1^{φ} indicate indel mutation effects on male- or female-specific DSB repair, potentially during spermatogenesis or oogenesis. Second, the reporter plasmid-based assay (Fig. 2) may not reflect full physiological DDRs in several aspects. (i) The induced DSBs may not require chromosome-associated regulation such as histone modifications and chromatin remodeling (Aleksandrov et al., 2020). (ii) As the nuclease-expressing plasmid was injected to the pre-blastoderm stage, a sufficient dose of the expressed nuclease may not be available in the early zygotic phase. (iii) The majority of DSB repair events scored at 48-hour of embryogenesis may be limited to somatic tissues. The germ cell unit is relatively a small portion, and any associated phenotype can be identified only after inheritance to offspring. (iv) DSB-associated phenotypes from pSSA may not reflect 100% of SSA-based DSB repair events because they can also be the result of either c-NHEJ or alt-EJ/MMEJ pathways. It is possible that indel mutations still shift the open reading frame of the luciferase maker gene or small-sized DR motifs might provide microhomology for an alternative process (McVey and Lee, 2008). We observed that indel mutation-related fluorescence changes were almost identical between both pNHEJ and pSSA reporters. Third, we also examined DNA repair events at the *kmo* locus of the *Ae. aegypti* genome by using CRISPR-based microinjection (Supplementary Fig. S3). Although an exogenous donor DNA was also included for ectopic HDR-mediated conversion into the genome, it was impossible to evaluate genetic mutation effects of NHEJ factors on HDR due to low homing-mediated transgenesis. Instead, their distinct effects on indel mutation occurrence (Supplementary Fig. S3B) were partly identified to supplement other assay results in this study. (i) Male offspring-specific increases of indels are associated with disruption of *ku80*. This may support the presence of an unknown end-joining mechanism identified in the reporter strain-based test (Fig. 4). (ii) Disruption of *lig4* critically decreased indels from G_0 offspring, indicating that it functions in DNA repair during the embryo development phases shown in assays using plasmid reporters (Fig. 2) and strain reporters (Fig. 5). (iii) A high rate of indels occurred only with *DNA-PKcs* heterozygosity, and this outcome was strengthened at G_1 offspring. This suggest that DNA-PKcs may play a homeostatic role in DNA repair during germline development (Fig. 6), but not in early embryos (Fig. 2).

Ae. aegypti Ku80 is a hierarchically dominant factor in DNA end joining mechanisms. In our reporter strain-based assay, the upsurge of indel mutations in the absence of Ku80 was

only observed through F_1 male offspring. This was not observed in plasmid-DSB repair tests nor through F_1 females, which shared the same genotypes and developmental stages with F_1 males. In addition, for CRISPR-induced DSBs on *kmo*, *ku80*$^{-/-}$ at G_0 mosquitoes also increased the indel scores in G_1 offspring. Thus, we presume that there is a male germline-specific mechanism to cope with DNA lesions occurring in spermatogenesis when the Ku-dependent pathway is abrogated. When c-NHEJ is defective or not completed (or KU is absent), the broken DNA ends are further degraded to produce a 3′-ssDNA overhang, and cells may switch DSB repair to alt-EJ (Mansour et al., 2013; Sallmyr and Tomkinson, 2018). The activation of alt-EJ was not detected when *lig4* or *DNA-PKcs* was deficient, consistent with a direct competition of Ku proteins and PARP-1 (Wang et al., 2006). This alternative mechanism or a regulatory signal may not be present in oogenesis, which might have hampered female fertility by *ku80* deficiency in this study.

Ae. aegypti DNA Ligase IV plays a core role in the NHEJ pathway. Our assays of reporter plasmids or CRISPR-targeted *kmo* revealed that dosages of the wild-type *lig4* gene were correlated to the rates of indel mutations. The *lig4*$^{-/-}$ strain showed the abrogation of DNA repair, while *lig4*$^{+/-}$ displayed an intermediate level of activity, suggesting that Lig4 may be a rate limiting NHEJ factor. Based upon test results in reporter strains, *lig4* contributes to NHEJ in an early embryonic phase, when zygotic formation and early cell division occur. In addition, *lig4*$^{-/-}$ contributed to DSB pathway bias toward SSA through F_1 females, potentially during female gametophyte development.

As a PI3KK, DNA-PKcs may have dual roles in DDRs. DNA-PKcs was known to interact with the C-terminal motif of Ku80 to form the DNA-PK holoenzyme complex (KU-DNA-PKcs) (Cary et al., 1997; Singleton et al., 1999), which then recruits and activates other factors at DSB sites (Shibata et al., 2011). While its kinase activity phosphorylates Artemis, XRCC4, Lig4, and XLF in favor of NHEJ (Davis et al., 2014), DNA-PKcs also reduces the kinase activity of ATM (Zhou et al., 2017) and alters the structure of the KU complex to lower its affinity to the broken DNA ends (Lee et al., 2015), which may stimulate MRN-dependent end resection (Deshpande et al., 2020). Our reporter plasmid-based test showed that either KU or Lig4-associated complex was indispensable for processing non-chromosomal DNA lesions in embryonic cells at somatic phases, but DNA-PKcs was not required. This result suggests that the KU complex achieves a flexible synapsis between two broken DNA ends, together with XRCC4/Lig4 only (Zhao et al., 2019). Meanwhile, in reporter strain-based tests, genetic disruption of DNA-PKcs increased SSA rates regardless of the nuclease-provider, father, or mother, indicating that its biasing effect was related to late phases of embryogenesis when germ units form. And *DNA-PKcs*$^{-/-}$ appeared to decrease NHEJ only through F_1 females, indicating its potential role in oogenesis. Meanwhile, in the assay with CRISPR-targeted *kmo*, an intermediate level of DNA-PKcs resulted in higher rates of NHEJ than either zero or the full dose did. Taken together, *Ae. aegypti* DNA-PKcs may be involved in homeostatic signaling to interlink diverse physiological DDRs (Yue et al., 2020).

In the current study, CRISPR-driven indel mutants of individual NHEJ factors (Ku80, Lig4, and DNA-PKcs) significantly modulated the DSB repair pathway bias according to cell types and developmental stages, proposing that NHEJ factors are potential candidates to

modulate efficiency of nuclease-based genome engineering in *Ae. aegypti*. Previously, the efficiency of ectopic HDR was shown to be elevated in embryos of *Drosophila* by a *lig4*-null mutation (Bozas et al., 2009), *Bombyx mori* by *Bmku70* knockout (Ma et al., 2014), and *Ae. aegypti* by the RNAi-inhibition of *ku70* (Basu et al., 2015). The inhibition of KU complex formation due to the absence of *ku80* or a delayed c-NHEJ process by *lig4* null-related stagnation may allow for the recruitment of competitors such as MRN/CtIP and PARP1 on the broken ends (Cheng et al., 2011; Wang et al., 2006), which accordingly influences pathway choice to process nuclease-induced local DNA lesions. According to our test results, individual NHEJ factors should be considered for their impacts on multiple aspects of gene editing and genetic control approaches. For example, CRISPR-based disruption of Ku80 activity or its dominant negative mutant can be explored to efficiently suppress c-NHEJ while it should be sufficient to compete with the uncharacterized alt-EJ mechanism, which can minimize indel alleles that are mainly responsible for the emergence of gene drive-resistant alleles. It is also noted that disrupting roles of *lig4* is predicted to have an effect on gene editing efficiency at early embryonic stages while targeting *DNA-PKcs* would do at post embryogenesis and early gametogenesis. While roles of key determining factors for the cell cycle (NHEJ available throughout all phases; HDR active only at S/G2) and extensive end resection (long ssDNA tails from the broken DNA ends) are emphasized for CRISPR/Cas9-mediated gene editing (Finney et al., 2022; Overcash et al., 2015; Scully et al., 2019), some critical machineries such as CtIP, XRCC4, RAD52, BRCA1, and PALB2 are yet to be identified in the *Ae. aegypti* genome (Mota et al., 2019). Further characterization of functional counterparts involved in DSB pathway choice are expected to advance nuclease-based gene drive technologies for vector mosquito species as well as contribute to our knowledge of eukaryotic DNA repair mechanisms.

Supplementary Material

Refer to Web version on PubMed Central for supplementary material.

Acknowledgements

We are grateful to members of the Adelman lab for technical support in rearing mosquitoes and preparing reagents/materials throughout the project.

Funding

This work was supported by the National Institute of Allergies and Infectious Diseases of the National Institutes of Health (NIH-NIAID) under award numbers [R01AI148787, R01AI137112], Texas A&M AgriLife Research under the Insect Vectored Disease Grant Program, and by the USDA National Institute of Food and Agriculture, Hatch project 1018401. The content is solely the responsibility of the authors and does not necessarily represent the official views of the National Institutes of Health or USDA.

Data availability

All data is included as supplemental information.

Abbreviations:

3′-ssDNA	3′-single-stranded DNA

53BP1	p53 binding protein 1
Alt-EJ/MMEJ	alternative end joining/microhomology-mediated end joining
BARD1	BRCA1-associated RING domain protein 1
BLM	Bloom syndrome protein RecQ family helicase
BRCA1/2	breast cancer type 1/2 susceptibility protein
CDK	cyclin-dependent kinase
CRISPR/Cas9	clustered regularly interspaced short palindromic repeats/ CRISPR-associated protein 9
CtIP	C terminus-binding protein-interacting protein
Dna2	DNA Replication Helicase/Nuclease 2 flap endonuclease
DDR	DNA damage response
DNA-PKcs	DNA-dependent protein kinase catalytic subunit
DSBs	DNA double-strand breaks
Exo1	5′-to-3′ exonuclease 1
HDR	homology-directed repair
HRMA	high-resolution melt analysis
Indels	nucleotide insertions or deletions
Lig1/3/4	DNA Ligase I/III/IV
MRN	MRE11-RAD50-NBS1
MRE11	meiotic recombination 11
NBS1	Nijmegen breakage syndrome protein 1
NHEJ	non-homologous end joining
PALB2	partner and localizer of BRCA2
PARP1	poly(ADP-ribose) polymerase 1
PI3KK	phosphatidylinositol 3-kinase-like serine/threonine protein kinases
Pol μ/λ/θ	DNA polymerases μ/λ/θ
RIF1	Rap1-interacting factor 1
RPA	replication protein A

SSA	single-strand annealing

References

Adelman ZN, Jasinskiene N, Onal S, Juhn J, Ashikyan A, Salampessy M, MacCauley T, James AA, 2007. Nanos gene control DNA mediates developmentally regulated transposition in the yellow fever mosquito Aedes aegypti. Proc. Natl. Acad. Sci. U. S. A 104, 9970–9975. 10.1073/pnas.0701515104. [PubMed: 17548819]

Aleksandrov R, Hristova R, Stoynov S, Gospodinov A, 2020. The chromatin response to double-strand DNA breaks and their repair. Cells. 10.3390/cells9081853.

Alhmoud JF, Woolley JF, Al Moustafa AE, Malki MI, 2020. DNA damage/repair management in cancers. Cancers (Basel). 10.3390/cancers12041050.

Alphey L, 2014. Genetic control of mosquitoes. Annu. Rev. Entomol 59, 205–224. 10.1146/annurev-ento-011613-162002. [PubMed: 24160434]

An L, Dong C, Li J, Chen J, Yuan J, Huang J, Chan KM, Yu CH, Huen MSY, 2018. RNF169 limits 53BP1 deposition at DSBs to stimulate single-strand annealing repair. Proc. Natl. Acad. Sci. U. S. A 115, E8286–E8295. 10.1073/pnas.1804823115. [PubMed: 30104380]

Aryan A, Anderson MAE, Myles KM, Adelman ZN, 2013a. TALEN-based gene disruption in the dengue vector Aedes aegypti. PLoS One 8, e60082. [PubMed: 23555893]

Aryan A, Anderson MAE, Myles KM, Adelman ZN, 2013b. Germline excision of transgenes in Aedes aegypti by homing endonucleases. Sci. Rep 3, 1603. 10.1038/srep01603. [PubMed: 23549343]

Basu S, Aryan A, Overcash JM, Samuel GH, Anderson MAE, Dahlem TJ, Myles KM, Adelman ZN, 2015. Silencing of end-joining repair for efficient site-specific gene insertion after TALEN/CRISPR mutagenesis in Aedes aegypti. Proc. Natl. Acad. Sci. U. S. A 112, 4038–4043. 10.1073/pnas.1502370112. [PubMed: 25775608]

Basu S, Aryan A, Haac ME, Myles KM, Adelman ZN, 2016. Methods for TALEN evaluation, use, and mutation detection in the mosquito Aedes aegypti. Methods Mol. Biol 1338, 157–177. 10.1007/978-1-4939-2932-0_13. [PubMed: 26443221]

Bétermier M, Bertrand P, Lopez BS, 2014. Is Non-Homologous End-Joining Really an Inherently Error-Prone Process? PLoS Genet. 10.1371/journal.pgen.1004086.

Bhargava R, Onyango DO, Stark JM, 2016. Regulation of Single-Strand Annealing and its Role in Genome Maintenance. Trends Genet. 10.1016/j.tig.2016.06.007.

Blum M, Chang HY, Chuguransky S, Grego T, Kandasaamy S, Mitchell A, Nuka G, Paysan-Lafosse T, Qureshi M, Raj S, Richardson L, Salazar GA, Williams L, Bork P, Bridge A, Gough J, Haft DH, Letunic I, Marchler-Bauer A, Mi H, Natale DA, Necci M, Orengo CA, Pandurangan AP, Rivoire C, Sigrist CJA, Sillitoe I, Thanki N, Thomas PD, Tosatto SCE, Wu CH, Bateman A, Finn RD, 2021. The InterPro protein families and domains database: 20 years on. Nucleic Acids Res. 49, D344–D354. 10.1093/nar/gkaa977. [PubMed: 33156333]

Bozas A, Beumer KJ, Trautman JK, Carroll D, 2009. Genetic analysis of zinc-finger nuclease-induced gene targeting in Drosophila. Genetics 182, 641–651. 10.1534/genetics.109.101329. [PubMed: 19380480]

Brouwer I, Sitters G, Candelli A, Heerema SJ, Heller I, Melo De AJ, Zhang H, Normanno D, Modesti M, Peterman EJG, Wuite GJL, 2016. Sliding sleeves of XRCC4-XLF bridge DNA and connect fragments of broken DNA. Nature 535, 566–569. 10.1038/nature18643. [PubMed: 27437582]

Cannavo E, Cejka P, 2014. Sae2 promotes dsDNA endonuclease activity within Mre11-Rad50-Xrs2 to resect DNA breaks. Nature 514, 122–125. 10.1038/nature13771. [PubMed: 25231868]

Canny MD, Moatti N, Wan LCK, Fradet-Turcotte A, Krasner D, Mateos-Gomez PA, Zimmermann M, Orthwein A, Juang YC, Zhang W, Noordermeer SM, Seclen E, Wilson MD, Vorobyov A, Munro M, Ernst A, Ng TF, Cho T, Cannon PM, Sidhu SS, Sicheri F, Durocher D, 2018. Inhibition of 53BP1 favors homology-dependent DNA repair and increases CRISPR-Cas9 genome-editing efficiency. Nat. Biotechnol 36, 95–102. 10.1038/nbt.4021. [PubMed: 29176614]

Cary RB, Peterson SR, Wang J, Bear DG, Bradbury EM, Chen DJ, 1997. DNA looping by Ku and the DNA-dependent protein kinase. Proc. Natl. Acad. Sci. U. S. A 94, 4267–4272. 10.1073/pnas.94.9.4267. [PubMed: 9113978]

Chae K, Dawson C, Valentin C, Contreras B, Zapletal J, Myles KM, Adelman ZN, 2022. Engineering a self-eliminating transgene in the yellow fever mosquito, Aedes aegypti. PNAS Nexus 1, pgac037. 10.1093/pnasnexus/pgac037. [PubMed: 36713320]

Chang HHY, Pannunzio NR, Adachi N, Lieber MR, 2017. Non-homologous DNA end joining and alternative pathways to double-strand break repair. Nat. Rev. Mol. Cell Biol 10.1038/nrm.2017.48.

Chen H, Lisby M, Symington LS, 2013. RPA Coordinates DNA End Resection and Prevents Formation of DNA Hairpins. Mol. Cell 50, 589–600. 10.1016/j.molcel.2013.04.032. [PubMed: 23706822]

Cheng Q, Barboule N, Frit P, Gomez D, Bombarde O, Couderc B, Ren GS, Salles B, Calsou P, 2011. Ku counteracts mobilization of PARP1 and MRN in chromatin damaged with DNA double-strand breaks. Nucleic Acids Res. 39, 9605–9619. 10.1093/nar/gkr656. [PubMed: 21880593]

Cornel AJ, Benedict MQ, Salazar Rafferty C, Howells AJ, Collins FH, 1997. Transient expression of the Drosophila melanogaster cinnabar gene rescues eye color in the white eye (WE) strain of Aedes aegypti. Insect Biochem. Mol. Biol 27, 993–997. 10.1016/S0965-1748(97)00084-2. [PubMed: 9569641]

Davis AJ, Chen BPC, Chen DJ, 2014. DNA-PK: A dynamic enzyme in a versatile DSB repair pathway. DNA Repair (Amst). 17, 21–29. 10.1016/j.dnarep.2014.02.020. [PubMed: 24680878]

Decottignies A, 2007. Microhomology-mediated end joining in fission yeast is repressed by pku70 and relies on genes involved in homologous recombination. Genetics 176, 1403–1415. 10.1534/genetics.107.071621. [PubMed: 17483423]

Deshpande RA, Myler LR, Soniat MM, Makharashvili N, Lee L, Lees-Miller SP, Finkelstein IJ, Paull TT, 2020. DNA-dependent protein kinase promotes DNA end processing by MRN and CtIP. Sci. Adv 6, eaay0922. 10.1126/sciadv.aay0922. [PubMed: 31934630]

DiCarlo JE, Chavez A, Dietz SL, Esvelt KM, Church GM, 2015. Safeguarding CRISPR-Cas9 gene drives in yeast. Nat. Biotechnol 33, 1250–1255. 10.1038/nbt.3412. [PubMed: 26571100]

Esvelt KM, Smidler AL, Catteruccia F, Church GM, 2014. Concerning RNA-guided gene drives for the alteration of wild populations. Elife 3, e03401. [PubMed: 25035423]

Fell VL, Schild-Poulter C, 2015. The Ku heterodimer: Function in DNA repair and beyond. Mutat. Res. - Rev. Mutat. Res 10.1016/j.mrrev.2014.06.002.

Finn RD, Coggill P, Eberhardt RY, Eddy SR, Mistry J, Mitchell AL, Potter SC, Punta M, Qureshi M, Sangrador-Vegas A, Salazar GA, Tate J, Bateman A, 2016. The Pfam protein families database: Towards a more sustainable future. Nucleic Acids Res. 44, D279–D285. 10.1093/nar/gkv1344. [PubMed: 26673716]

Finney M, Romanowski J, Adelman ZN, 2022. Strategies to improve homology-based repair outcomes following CRISPR-based gene editing in mosquitoes: lessons in how to keep any repair disruptions local. Virol. J 19, 128. 10.1186/s12985-022-01859-2. [PubMed: 35908059]

Gantz VM, Bier E, 2015. The mutagenic chain reaction: A method for converting heterozygous to homozygous mutations. Science 348, 442–444. 10.1126/science.aaa5945. [PubMed: 25908821]

Gantz VM, Jasinskiene N, Tatarenkova O, Fazekas A, Macias VM, Bier E, James AA, 2015. Highly efficient Cas9-mediated gene drive for population modification of the malaria vector mosquito Anopheles stephensi. Proc. Natl. Acad. Sci. U. S. A 112, E6736–E6743. 10.1073/pnas.1521077112. [PubMed: 26598698]

Gibson BA, Kraus WL, 2012. New insights into the molecular and cellular functions of poly(ADP-ribose) and PARPs. Nat. Rev. Mol. Cell Biol 10.1038/nrm3376.

Goodarzi AA, Yu Y, Riballo E, Douglas P, Walker SA, Ye R, Härer C, Marchetti C, Morrice N, Jeggo PA, Lees-Miller SP, 2006. DNA-PK autophosphorylation facilitates Artemis endonuclease activity. EMBO J. 25, 3880–3889. 10.1038/sj.emboj.7601255. [PubMed: 16874298]

Grawunder U, Wilm M, Wu X, Kulesza P, Wilson TE, Mann M, Lieber MR, 1997. Activity of DNA ligase IV stimulated by complex formation with XRCC4 protein in mammalian cells. Nature 388, 492–495. 10.1038/41358. [PubMed: 9242410]

Han Q, Calvo E, Marinotti O, Fang J, Rizzi M, James AA, Li J, 2003. Analysis of the wild-type and mutant genes encoding the enzyme kynurenine monooxygenase of the yellow fever mosquito. Aedes aegypti. Insect Mol. Biol 12, 483–490. 10.1046/j.1365-2583.2003.00433.x. [PubMed: 12974953]

Huang RX, Zhou PK, 2020. DNA damage response signaling pathways and targets for radiotherapy sensitization in cancer. Signal Transduct. Target. Ther 10.1038/s41392-020-0150-x.

Jackson SP, Bartek J, 2009. The DNA-damage response in human biology and disease. Nature. 10.1038/nature08467.

Jeggo PA, Pearl LH, Carr AM, 2016. DNA repair, genome stability and cancer: A historical perspective. Nat. Rev. Cancer 10.1038/nrc.2015.4.

KaramiNejadRanjbar M, Eckermann KN, Ahmed HMM, Héctor Sánchez CM, Dippel S, Marshall JM, Wimmer EA, 2018. Consequences of resistance evolution in a Cas9-based sex conversion-suppression gene drive for insect pest management. Proc. Natl. Acad. Sci. U. S. A 115, 6189–6194. 10.1073/pnas.1713825115. [PubMed: 29844184]

Kistler KE, Vosshall LB, Matthews BJ, 2015. Genome engineering with CRISPRCas9 in the mosquito Aedes aegypti. Cell Rep. 11, 51–60. 10.1016/j.celrep.2015.03.009. [PubMed: 25818303]

Lee KJ, Saha J, Sun J, Fattah KR, Wang SC, Jakob B, Chi L, Wang SY, Taucher-Scholz G, Davis AJ, Chen DJ, 2015. Phosphorylation of Ku dictates DNA double-strand break (DSB) repair pathway choice in S phase. Nucleic Acids Res. 44, 1732–1745. 10.1093/nar/gkv1499. [PubMed: 26712563]

Liu T, Huang J, 2016. DNA End Resection: Facts and Mechanisms. Genomics, Proteomics Bioinforma. 10.1016/j.gpb.2016.05.002.

Ma S, Chang J, Wang X, Liu Y, Zhang J, Lu W, Gao J, Shi R, Zhao P, Xia Q, 2014. CRISPR/Cas9 mediated multiplex genome editing and heritable mutagenesis of BmKu70 in Bombyx mori. Sci. Rep 4, 4489. 10.1038/srep04489. [PubMed: 24671069]

Mansour WY, Borgmann K, Petersen C, Dikomey E, Dahm-Daphi J, 2013. The absence of Ku but not defects in classical non-homologous end-joining is required to trigger PARP1-dependent end-joining. DNA Repair (Amst). 12, 1134–1142. 10.1016/j.dnarep.2013.10.005. [PubMed: 24210699]

Marini F, Rawal CC, Liberi G, Pellicioli A, 2019. Regulation of DNA Double Strand Breaks Processing: Focus on Barriers. Front. Mol. Biosci 10.3389/fmolb.2019.00055.

Masani S, Han L, Meek K, Yu K, 2016. Redundant function of DNA ligase 1 and 3 in alternative end-joining during immunoglobulin class switch recombination. Proc. Natl. Acad. Sci. U. S. A 113, 1261–1266. 10.1073/pnas.1521630113. [PubMed: 26787901]

Mateos-Gomez PA, Gong F, Nair N, Miller KM, Lazzerini-Denchi E, Sfeir A, 2015. Mammalian polymerase θ promotes alternative NHEJ and suppresses recombination. Nature 518, 254–257. 10.1038/nature14157. [PubMed: 25642960]

McElhinny SAN, Havener JM, Garcia-Diaz M, Juárez R, Bebenek K, Kee BL, Blanco L, Kunkel TA, Ramsden DA, 2005. A gradient of template dependence defines distinct biological roles for family X polymerases in nonhomologous end joining. Mol. Cell 19, 357–366. 10.1016/j.molcel.2005.06.012. [PubMed: 16061182]

McVey M, Lee SE, 2008. MMEJ repair of double-strand breaks (director's cut): deleted sequences and alternative endings. Trends Genet. 10.1016/j.tig.2008.08.007.

Mota MBS, Carvalho MA, Monteiro ANA, Mesquita RD, 2019. DNA damage response and repair in perspective: Aedes aegypti, Drosophila melanogaster and Homo sapiens. Parasites and Vectors. 10.1186/s13071-019-3792-1.

Motycka TA, Bessho T, Post SM, Sung P, Tomkinson AE, 2004. Physical and Functional Interaction between the XPF/ERCC1 Endonuclease and hRad52. J. Biol. Chem 279, 13634–13639. 10.1074/jbc.M313779200. [PubMed: 14734547]

Nimonkar AV, Genschel J, Kinoshita E, Polaczek P, Campbell JL, Wyman C, Modrich P, Kowalczykowski SC, 2011. BLM-DNA2-RPA-MRN and EXO1-BLMRPA-MRN constitute two DNA end resection machineries for human DNA break repair. Genes Dev. 25, 350–362. 10.1101/gad.2003811. [PubMed: 21325134]

Ovejero S, Bueno A, Sacristán MP, 2020. Working on genomic stability: From the S-phase to mitosis. Genes (Basel). 10.3390/genes11020225.

Overcash JM, Aryan A, Myles KM, Adelman ZN, 2015. Understanding the DNA damage response in order to achieve desired gene editing outcomes in mosquitoes. Chromosom. Res 23, 31–42. 10.1007/s10577-014-9450-8.

Pommier Y, Sun Y, Huang SYN, Nitiss JL, 2016. Roles of eukaryotic topoisomerases in transcription, replication and genomic stability. Nat. Rev. Mol. Cell Biol 10.1038/nrm.2016.111.

Raban RR, Marshall JM, Akbari OS, 2020. Progress towards engineering gene drives for population control. J. Exp. Biol 10.1242/jeb.208181.

Sallmyr A, Tomkinson AE, 2018. Repair of DNA double-strand breaks by mammalian alternative end-joining pathways. J. Biol. Chem 10.1074/jbc.TM117.000375.

Sartori AA, Lukas C, Coates J, Mistrik M, Fu S, Bartek J, Baer R, Lukas J, Jackson SP, 2007. Human CtIP promotes DNA end resection. Nature 450, 509–514. 10.1038/nature06337. [PubMed: 17965729]

Scully R, Panday A, Elango R, Willis NA, 2019. DNA double-strand break repair-pathway choice in somatic mammalian cells. Nat. Rev. Mol. Cell Biol 10.1038/s41580-019-0152-0.

Shibata A, Conrad S, Birraux J, Geuting V, Barton O, Ismail A, Kakarougkas A, Meek K, Taucher-Scholz G, Löbrich M, Jeggo PA, 2011. Factors determining DNA double-strand break repair pathway choice in G2 phase. EMBO J. 30, 1079–1092. 10.1038/emboj.2011.27. [PubMed: 21317870]

Shibata A, Moiani D, Arvai AS, Perry J, Harding SM, Genois MM, Maity R, van Rossum-Fikkert S, Kertokalio A, Romoli F, Ismail A, Ismalaj E, Petricci E, Neale MJ, Bristow RG, Masson JY, Wyman C, Jeggo PA, Tainer JA, 2014. DNA Double-Strand Break Repair Pathway Choice Is Directed by Distinct MRE11 Nuclease Activities. Mol. Cell 53, 7–18. 10.1016/j.molcel.2013.11.003. [PubMed: 24316220]

Singleton BK, Torres-Arzayus MI, Rottinghaus ST, Taccioli GE, Jeggo PA, 1999. The C terminus of Ku80 activates the DNA-dependent protein kinase catalytic subunit. Mol. Cell. Biol 19, 3267–3277. 10.1128/mcb.19.5.3267. [PubMed: 10207052]

Soulas-Sprauel P, Rivera-Munoz P, Malivert L, Le Guyader G, Abramowski V, Revy P, De Villartay JP, 2007. V(D)J and immunoglobulin class switch recombinations: A paradigm to study the regulation of DNA end-joining. Oncogene. 10.1038/sj.onc.1210875.

Sun Y, McCorvie TJ, Yates LA, Zhang X, 2020. Structural basis of homologous recombination. Cell. Mol. Life Sci 10.1007/s00018-019-03365-1.

Symington LS, Gautier J, 2011. Double-strand break end resection and repair pathway choice. Annu. Rev. Genet 45, 247–271. 10.1146/annurev-genet-110410-132435. [PubMed: 21910633]

Tsujimoto H, Adelman ZN, 2021. Improved fecundity and fertility assay for Aedes aegypti using 24 well tissue culture plates (EAgaL plates). J. Vis. Exp 10.3791/61232.

Untergasser A, Cutcutache I, Koressaar T, Ye J, Faircloth BC, Remm M, Rozen SG, 2012. Primer3-new capabilities and interfaces. Nucleic Acids Res. 40 10.1093/nar/gks596.

Walker JR, Corpina RA, Goldberg J, 2001. Structure of the Ku heterodimer bound to dna and its implications for double-strand break repair. Nature 412, 607–614. 10.1038/35088000. [PubMed: 11493912]

Wang M, Wu W, Wu W, Rosidi B, Zhang L, Wang H, Iliakis G, 2006. PARP-1 and Ku compete for repair of DNA double strand breaks by distinct NHEJ pathways. Nucleic Acids Res. 34, 6170–6182. 10.1093/nar/gkl840. [PubMed: 17088286]

Winterbourn CC, 2008. Reconciling the chemistry and biology of reactive oxygen species. Nat. Chem. Biol 10.1038/nchembio.85.

Wu P-Y, Frit P, Meesala S, Dauvillier S, Modesti M, Andres SN, Huang Y, Sekiguchi J, Calsou P, Salles B, Junop MS, 2009. Structural and Functional Interaction between the Human DNA Repair Proteins DNA Ligase IV and XRCC4. Mol. Cell. Biol 29, 3163–3172. 10.1128/mcb.01895-08. [PubMed: 19332554]

Yue X, Bai C, Xie D, Ma T, Zhou PK, 2020. DNA-PKcs: A multi-faceted player in DNA damage response. Front. Genet 10.3389/fgene.2020.607428.

Zapletal J, Najmitabrizi N, Erraguntla M, Lawley MA, Myles KM, Adelman ZN, 2021. Making gene drive biodegradable. Philos. Trans. R. Soc. Lond. B. Biol. Sci 376, 20190804. 10.1098/rstb.2019.0804. [PubMed: 33357058]

Zhao B, Watanabe G, Morten MJ, Reid DA, Rothenberg E, Lieber MR, 2019. The essential elements for the noncovalent association of two DNA ends during NHEJ synapsis. Nat. Commun 10, 3588. 10.1038/s41467-019-11507-z. [PubMed: 31399561]

Zhou Y, Lee JH, Jiang W, Crowe JL, Zha S, Paull TT, 2017. Regulation of the DNA damage response by DNA-PKcs inhibitory phosphorylation of ATM. Mol. Cell 65, 91–104. 10.1016/j.molcel.2016.11.004. [PubMed: 27939942]

Zuker M, 2003. Mfold web server for nucleic acid folding and hybridization prediction. Nucleic Acids Res. 31 10.1093/nar/gkg595.

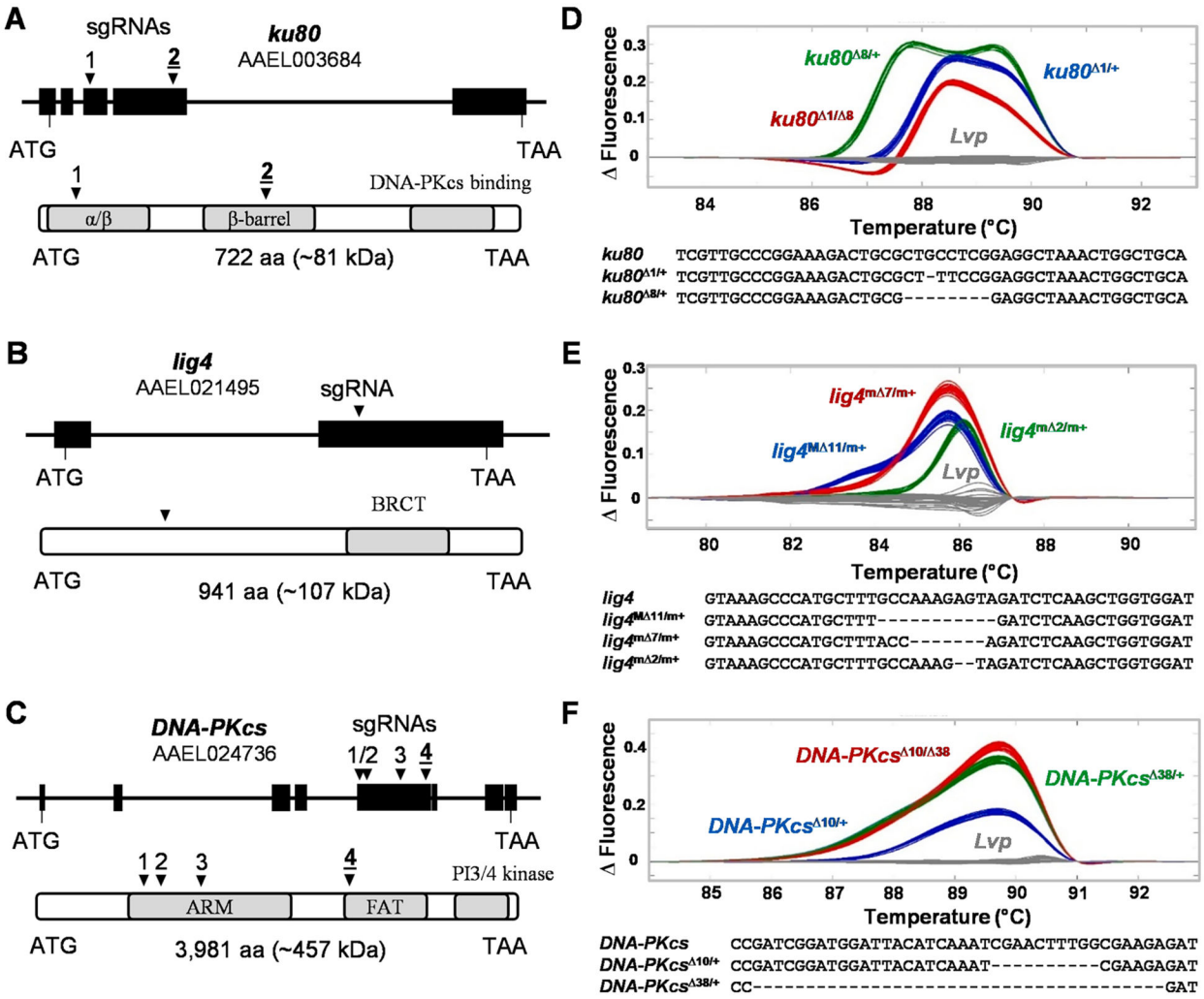

Fig. 1.

Generation of CRISPR/Cas9-driven indel mutant mosquitoes for NHEJ-associated genes in *Ae. aegypti*. Schematic representation of the *Ae. aegypti ku80* **(A)**, *lig4* (**B**), and *DNA-PKcs* (**C**) genes and corresponding predicted proteins. For all, arrowheads indicate the target sites of initial sgRNA groups. sgRNA groups selected for germline mutagenesis are underlined. Differential melting curve patterns of *ku80* (G_6 generation) (**D**), *lig4* (G_5 generation) (**E**), and *DNA-PKcs* (G_6 generation) (**F**). For all samples, Δ indicates nucleotide deletion and + indicates the wild-type allele; superscript M/m indicates the M/m-sex chromosome-like regions in *Ae. aegypti*.

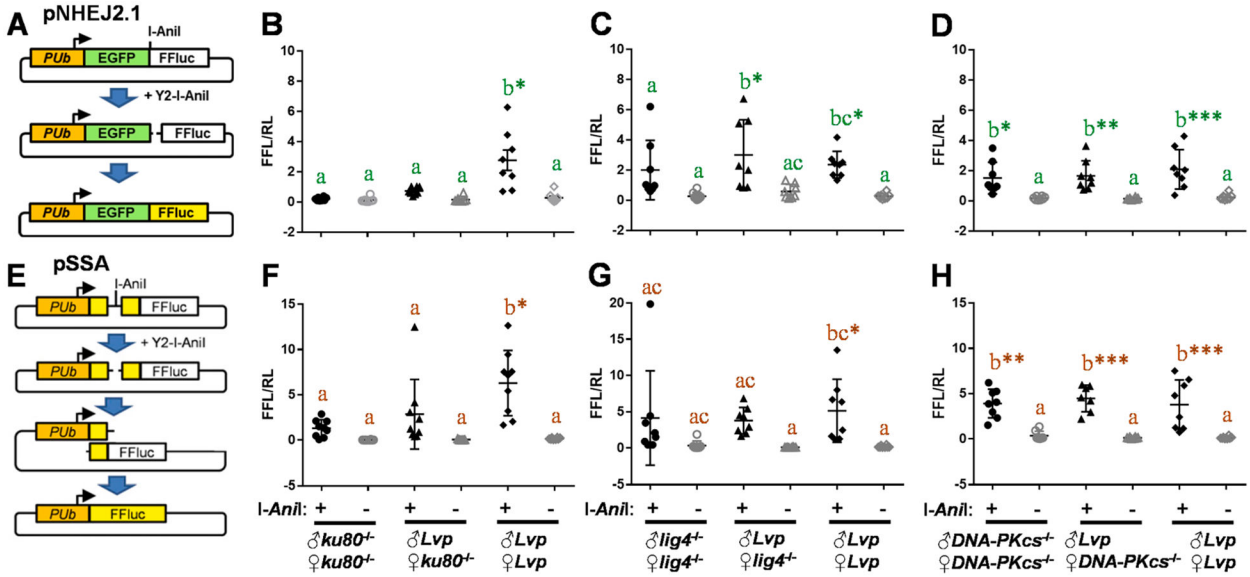

Fig. 2.

Plasmid-based DNA repair assays in NHEJ-associated gene mutant embryos. Two luciferase reporter plasmids, pNHEJ2.1 (**A**) and pSSA (**E**), were tested for effects of NHEJ gene disruption on DNA double-strand breaks (DSBs) in *Ae. aegypti*. For NHEJ- (**B** to **D**) or SSA-based (**F** to **H**) DNA repair assays, each reporter plasmid was microinjected with the I-*Ani*I-expressing or control plasmid to pre-blastoderm embryos in 8 replicates (50 embryos per each) obtained from crosses between the *trans*-heterozygous indel mutant ($ku80^{-/-}$, $lig4^{-/-}$, or $DNA\text{-}PKcs^{-/-}$) and *Lvp* strains. The dual-luciferase assay was performed 48-hour post injection to measure NHEJ- or SSA-dependent luciferase reporter activity with normalization by the level of Renilla luciferase. Letters indicate statistically separate groups, and stars indicate significance of difference in between + I-*Ani*I and -I-*Ani*I groups. Tukey's multiple comparison test (One-way ANOVA): ***, $P < 0.001$; **, $P < 0.01$; *, $P < 0.05$.

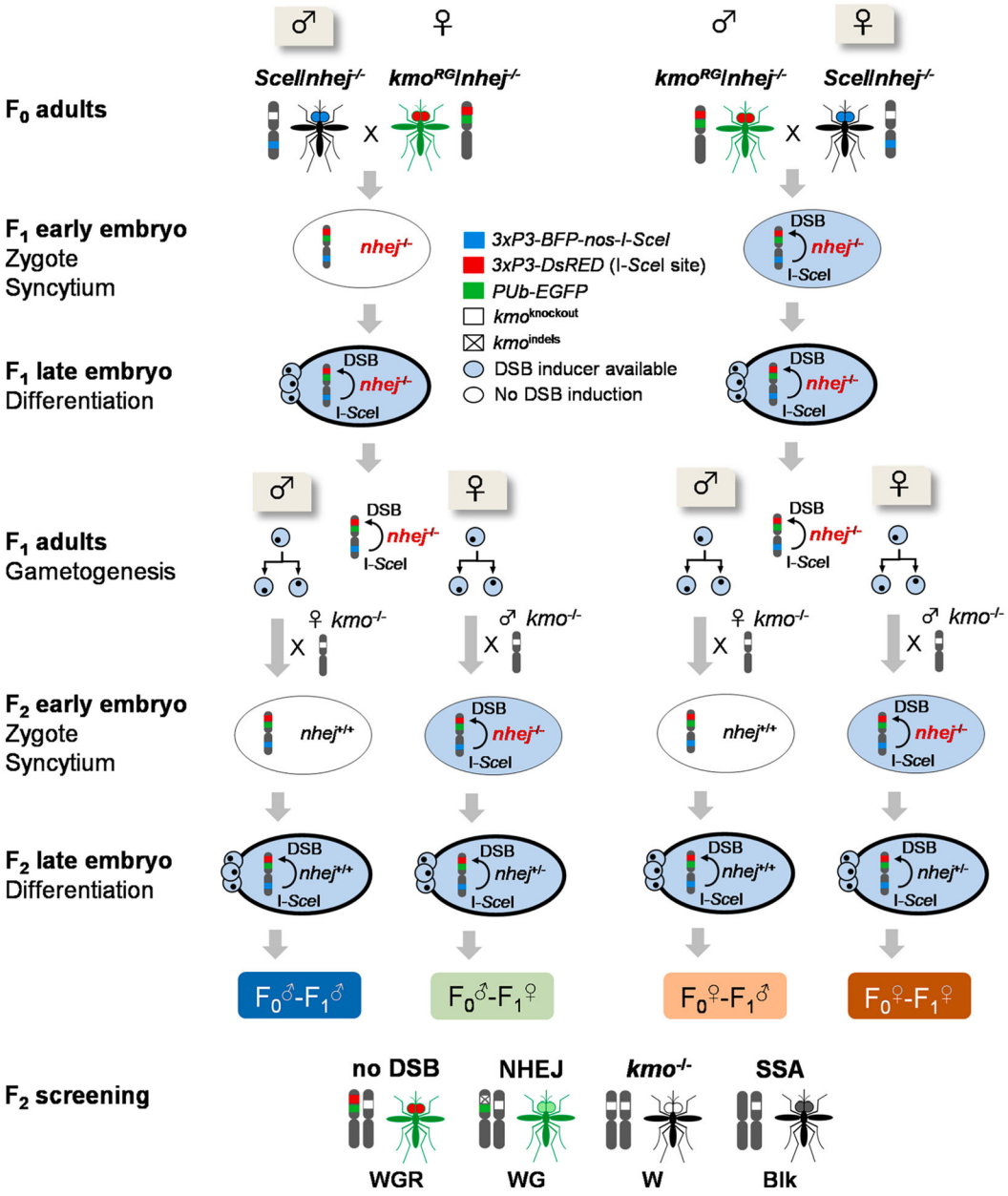

Fig. 3.

Developmental and molecular schematics of nuclease-induced DSBs and potential repair outcomes in the absence of wild-type NHEJ genes. Following crossing between the reporter (*kmo*^{RG}/*nhej*$^{-/-}$) and nuclease (*SceI*/*nhej*$^{-/-}$) strains, the F_1 offspring (*SceI*/*kmo*^{RG}/*nhej*$^{-/-}$) were outcrossed to *kmo*$^{-/-}$. F_2 mosquitoes were scored for marker phenotypes, which are dependent on DNA repair pathway selected for repairing I-*Sce*I-induced DSBs: WGR (Kmo-; EGFP+; DsRED +) for no DSB; WG (Kmo-; EGFP+; DsRED-) for NHEJ-mediated indel mutation; W (Kmo-; EGFP-; DsRED-) for the *kmo*-null allele; Blk (Kmo+; EGFP-; DsRED-) for SSA-mediated transgene elimination. The DNA repair-associated phenotypes were scored for each F_2 group, which had distinct heritage of the DSB-inducing nuclease

based on the presence/absence of maternally contributed I-*Sce*I: [$F_0^{\male} - F_1^{\male}$], [$F_0^{\male} - F_1^{\female}$], [$F_0^{\female} - F_1^{\male}$], and [$F_0^{\female} - F_1^{\female}$].

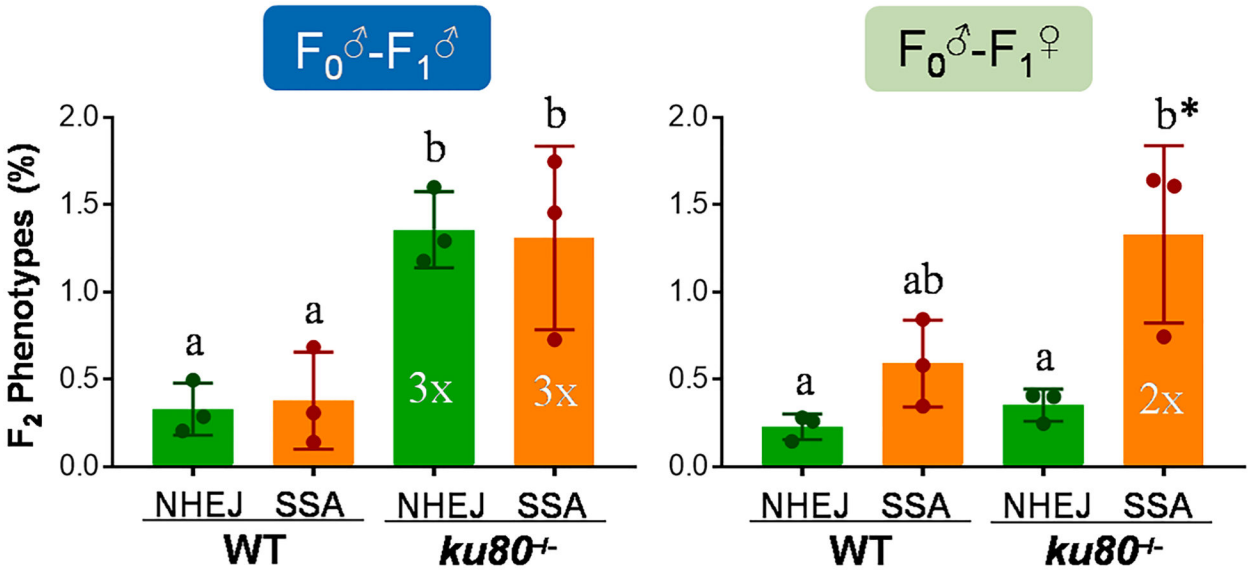

Fig. 4.

Effects of *Ae. aegypti ku80* disruption on SSA and NHEJ based repair of a chromosomally integrated reporter. The F_2 offspring groups (triplicate) were scored for DNA repair pathway-dependent marker phenotypes: WG (Kmo-; EGFP+; DsRED-) for NHEJ [% WG/(WGR + WG + Blk)]; Blk (Kmo+; EGFP-; DsRED-) for SSA [% Blk/(WGR + WG + Blk)]. The labels of $F_0^x - F_1^x$ indicate the lineage of *nos-I-SceI* (the DSB-inducing nuclease) of the F_2 offspring group. Letters indicate statistically identical/different groups; stars indicate significance between NHEJ and SSA. Numeric values on the columns indicate fold differences in between $ku80^{-/-}$ and WT. Tukey's multiple comparison test (One-way ANOVA): $P < 0.05$.

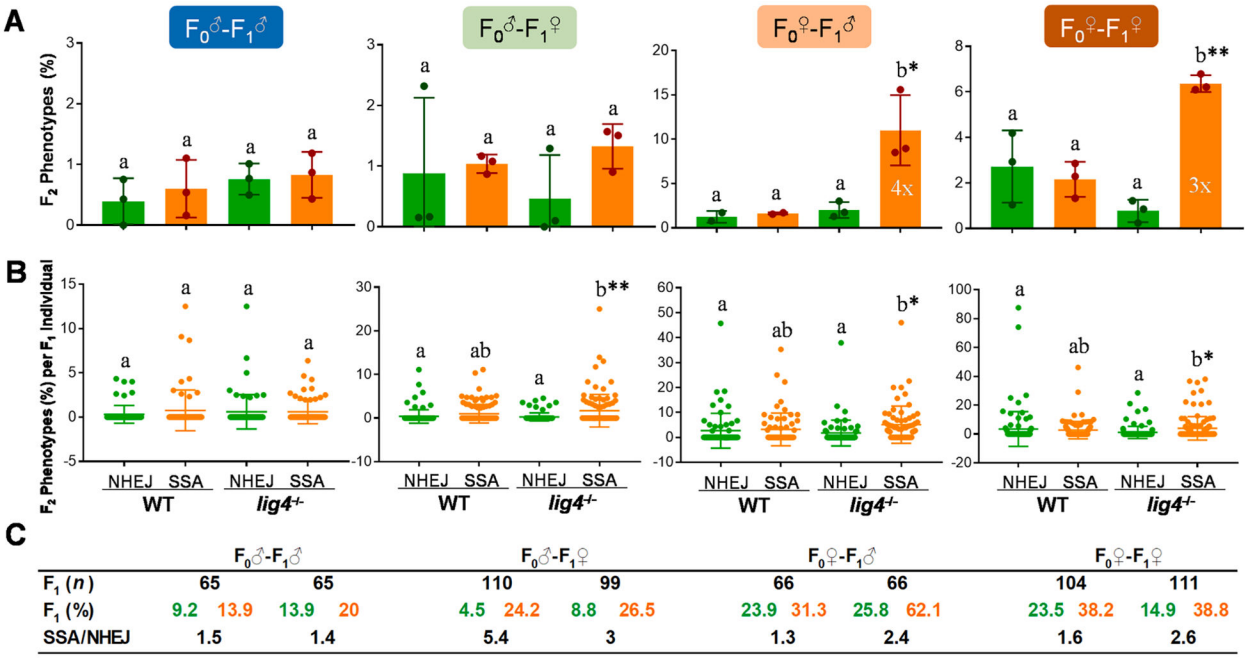

	F0♂-F1♂		F0♂-F1♀		F0♀-F1♂		F0♀-F1♀	
F1 (*n*)	65	65	110	99	66	66	104	111
F1 (%)	9.2 13.9	13.9 20	4.5 24.2	8.8 26.5	23.9 31.3	25.8 62.1	23.5 38.2	14.9 38.8
SSA/NHEJ	1.5	1.4	5.4	3	1.3	2.4	1.6	2.6

Fig. 5.

Effects of *Ae. aegypti lig4* disruption on SSA and NHEJ based repair of a chromosomally integrated reporter. (**A**) F_2 offspring (triplicate groups) were scored for DNA repair pathway-dependent marker phenotypes: WG (Kmo-; EGFP+; DsRED-) for NHEJ [% WG/(WGR + WG + Blk)]; Blk (Kmo+; EGFP-; DsRED-) for SSA [% Blk/(WGR + WG + Blk)]. The labels of $F_0^x - F_1^x$ indicate the lineage of *nos-I-SceI* (the DSB-inducing nuclease) of the F_2 offspring group. Letters indicate statistically identical/different groups, and stars indicate significance of difference in between NHEJ and SSA. Numeric values on the columns indicate fold differences in between *lig4*$^{-/-}$ and WT. Tukey's multiple comparison test (One-way ANOVA): $P < 0.05$. (**B**) DNA repair pathway-dependent marker phenotypes of F_2 progeny were scored per individual F_1 female. Each dot represents rates of NHEJ and SSA events recovered in the progeny of a single F_1 female. Tukey's multiple comparison test (One-way ANOVA): $P < 0.05$. (**C**) The total # of F1 founders [F1 (n)], the percentage of founders that produced at least one NHEJ (green) or SSA (orange) progeny [F1 (%)], and the ratio of the number of founders that produced at least one SSA event versus those that produced at least one NHEJ event (note that founders that produced both types of events would be counted in both).

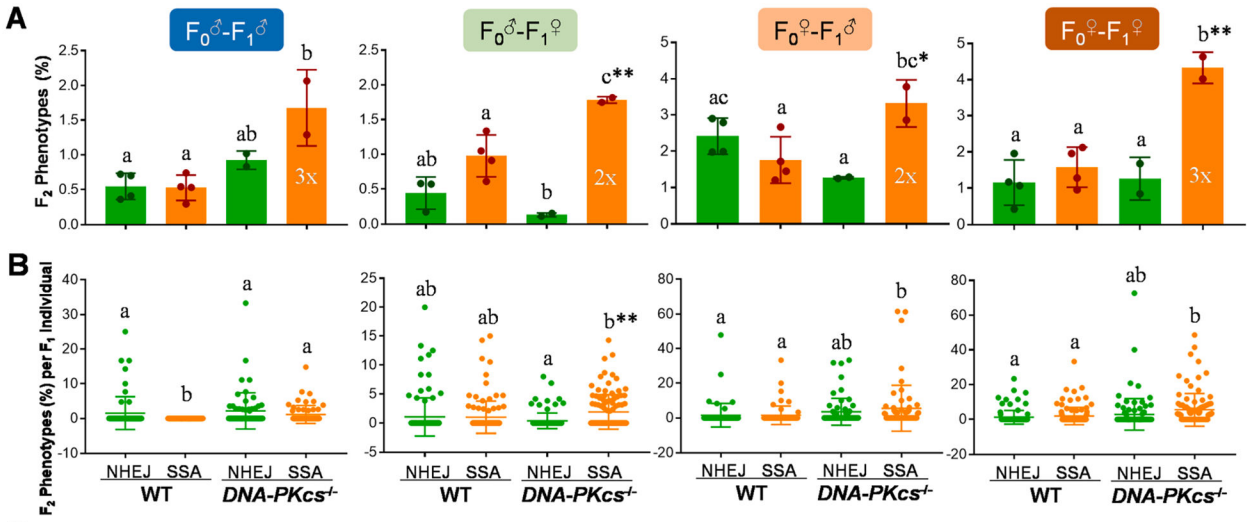

Fig. 6.

Effects of *Ae. aegypti DNA-PKcs* disruption on SSA and NHEJ based repair of a chromosomally integrated reporter. (**A**) F_2 offspring (triplicate groups) were scored for DNA repair pathway-dependent marker phenotypes: WG (Kmo-; EGFP+; DsRED-) for NHEJ [% WG/(WGR + WG + Blk)]; Blk (Kmo+; EGFP-; DsRED-) for SSA [% Blk/(WGR + WG + Blk)]. The labels of $F_0^x - F_1^x$ indicate the lineage of *nos-I-SceI* (the DSB-inducing nuclease) of the F_2 offspring group. Letters indicate statistically identical/different groups, and stars indicate significance of difference in between NHEJ and SSA. Numeric values on the columns indicate fold differences in between *DNA-PKcs*$^{-/-}$ and WT. Tukey's multiple comparison test (One-way ANOVA): $P < 0.05$. (**B**) DNA repair pathway-dependent marker phenotypes of F_2 progeny were scored per individual F_1 female. Each dot represents rates of NHEJ and SSA events recovered in the progeny of a single F_1 female. Tukey's multiple comparison test (One-way ANOVA): $P < 0.05$. (**C**) The total # of F_1 founders [F_1 (*n*)], the percentage of founders that produced at least one NHEJ (green) or SSA (orange) progeny [F_1 (%)], and the ratio of the number of founders that produced at least one SSA event versus those that produced at least one NHEJ event (note that founders that produced both types of events would be counted in both).

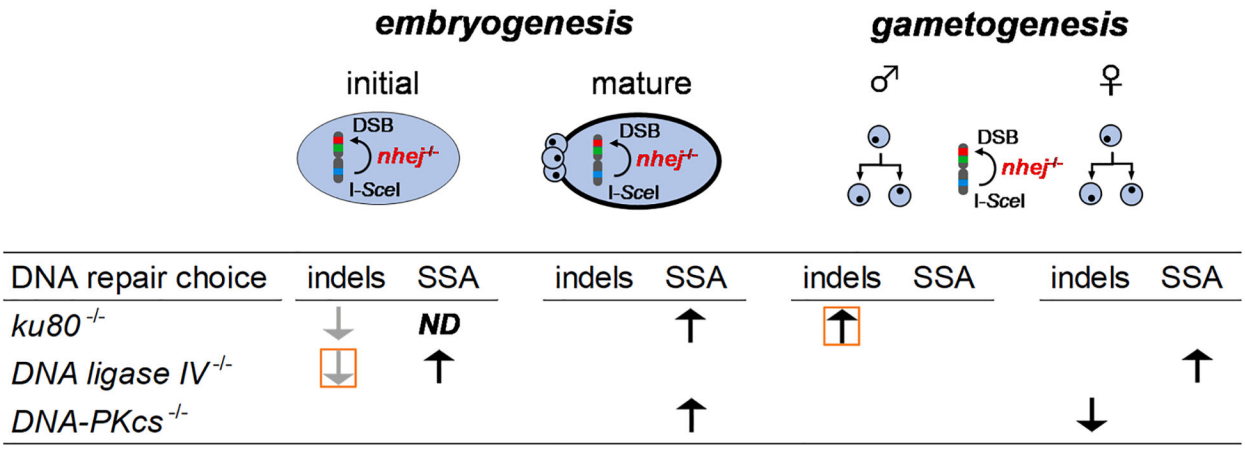

Fig. 7.

Various effects of NHEJ-associated gene disruption on nuclease-driven DSBs in the self-eliminating transgene engineered in the *Ae. aegypti* genome. How the deficiency of individual NHEJ factor could influence DNA repair pathway selection was summarized with respect to somatic or germline tissues in the development of *Ae. aegypti*. The initial embryos may include DNA repair mechanisms occurred in zygotic or syncytial blastoderm stages, and the mature embryos in cellular differentiation or gastrulation stages. The late embryogenesis may include the germline unit formation, and adult mosquitoes may represent DNA repair events in male spermatogenesis and female oogenesis. Upward arrows indicate the enhancement of DNA repair pathway outcomes due to genetic mutations in individual NHEJ genes; Downward arrows indicate the suppression; Gray-colored arrows indicate genetic mutation effects specifically obtained from the reporter plasmid-based assay; Red square boxes indicate effects supported by the kmo-targeted DNA repair assay; *ND*, not determined.

Table 1

Development of CRISPR/Cas9-driven indel mutant strains for non-homologous end joining (NHEJ)-associated genes in the *Ae. aegypti* genome.

Genes	sgRNA sites (3 DSBs per site)	DSB-inducing activity	# Embryos injected	# G_0 Larvae survived (Survival Rate)	G_1 Indel mutants obtained[a]
ku80 (AAEL003684)	ku80 #1	+	*NA*	*NA*	*NA*
	ku80 #2	+++	~400	8 (2%)	Δ**8**
			~400	47 (11.8%)	Δ**1**
lig4 (AAEL021495)	lig4–3	*ND*	~400	91 (22.8%)	$\Delta 7^{M}$, $\Delta \mathbf{11^{M}}$
					$\Delta \mathbf{2^{m}}$, $\Delta 5^{m}$, $\Delta \mathbf{7^{m}}$
DNA-PKcs (AAEL024736)	DNA-PKcs #1	++	~400	21 (5%)	None
	DNA-PKcs #2	–	*NA*	*NA*	*NA*
	DNA-PKcs #3	+++	~450	104 (23.1%)	Δ7
	DNA-Pkcs #4	+++	~400	89 (22.3%)	Δ**10**; Δ**38**; +5

a, Δ indicates nucleotide deletion; + indicates nucleotide insertion. Superscripts indicate the M/m-locus, a sex chromosome-like region in *Ae. aegypti*. Bold letters indicate indel mutations characterized for their phenotypes in this study. *NA*, not applicable. *ND*, not determined.